

Ab initio configuration interaction calculations of the semiconductor ternary clusters $\text{Ge}_l\text{Si}_m\text{C}_n$ ($l+m+n \leq 6$)

Si-Dian Li,^{1,2} Sheng-Yun Li,³ Ming-Gen Zhao,² Hai-Shun Wu,⁴ and Zhi-Hao Jin¹¹*School of Materials Science and Engineering, Xian Jiaotong University, Xian 710049, People's Republic of China*²*Department of Chemistry, Xinzhou Teachers' University, Xinzhou 034000, Shanxi, People's Republic of China*³*Department of Chemistry, Taiyuan Teachers' College, Taiyuan 030001, People's Republic of China*⁴*Institute of Materials Chemistry, Shanxi Normal University, Linfen 041000, Shanxi, People's Republic of China*

(Received 15 February 2002; revised manuscript received 30 May 2002; published 23 October 2002)

Ground-state structures, stabilization energies, HOMO-LUMO energy gaps, and vibrational frequencies of $\text{Ge}_l\text{Si}_m\text{C}_n$ ternary microclusters ($s=l+m+n \leq 6$) have been investigated using the configuration interaction with all single and double substitutions method, and ionization potentials and vertical detachment energies of trimers and tetramers predicted utilizing the outer valence Green-function frozen-core procedure. $\text{Ge}_l\text{Si}_m\text{C}_n$ is found to follow structural patterns similar to corresponding $\text{Si}_{l+m}\text{C}_n$ binary clusters and most ternary species possess singlet ground states except GeSiC_4 , which prefers a triplet one. Trimers, tetramers, and GeSi_2C_2 are planar, and the C-rich GeSiC_3 and GeSiC_4 are linear, while all the other Si-rich or Si- and Ge-rich clusters with $s \geq 5$ atoms prefer three-dimensional structures. Formation of strong C=C bond(s) predominates the relative stabilities of different isomers for clusters with limited numbers of C atoms, while Si=C bonds play an important role for silicon-rich species or systems with close C and Si atomic ratios. Planar and linear semiconductor clusters possess delocalized multicenter-two-electron π bonds (aromatic) and follow the $(4n+2)$ electron counting rule. Frequency analyses indicate that most vibrational modes of small ternary clusters are carbon dominated in terms of amplitudes, while Si atoms vibrate in medium sizes and Ge atoms vibrate very weakly.

DOI: 10.1103/PhysRevB.66.165213

PACS number(s): 73.22.-f, 61.46.+w

I. INTRODUCTION

Extensive research has been focused on group-IV A elemental clusters C_n , Si_n , Ge_n , Sn_n , and Pb_n in the past two decades for both fundamental and technological reasons, while very limited experimental and theoretical investigations performed on binary A_mB_n or ternary $A_lB_mC_n$ clusters ($A, B, C = \text{C, Si, and Ge}$).¹⁻¹⁰ In applications, however, binary SiC bulks are important ceramics and possible wide-gap semiconductor materials and binary GeSi and ternary GeSiC thin films deposited on Si substrates have generated a new generation of high performance heterojunction bipolar transistors.³ In-depth studies on binary A_nB_m and ternary $A_lB_mC_n$ semiconductor microclusters will reveal properties of the bulk materials and shed insight into the clustering processes in the gas phase during depositions under various conditions.

Over the past several years, Froudakis and co-workers have performed various *ab initio* investigations on Si_mC_n binary microclusters, including the second-order Moller-Plesset (MP2) and coupled cluster singles and doubles (CCSD) calculations on Si_4C_4 ,⁴ MP2 or higher-order perturbation (CASP2) on Si_2C_4 , Si_3C_3 , and Si_2C_4 ,^{5,6} MP2 and CCSD(T) on Si_3C_2 ,⁷ and CCSD(T) and tight-binding molecular-dynamics studies on SiGe, Si_2Ge_2 , and Si_2Ge_4 .¹ Earlier theoretical and experimental investigations provided detailed structural and bonding characteristics for Si_2C (Ref. 8) and Si_2C_2 .^{9,10} Very recently, we presented a density-functional theory (DFT) study on binary microclusters A_mB_n ($A, B = \text{Si, Ge}; s = m + n \leq 10$) (Ref. 2) and found that these clusters follow similar structural patterns to corresponding

elemental Si_s and Ge_s ,¹¹ and have more isomers with lower symmetries. However, as we know, there have been no theoretical or experimental results reported on $\text{Ge}_l\text{Si}_m\text{C}_n$ ternary clusters to date.

In this work, we present *ab initio* configuration interaction calculations on $\text{C}_l\text{Si}_m\text{Ge}_n$ ternary microclusters ($s=l+m+n \leq 6$). Compared to elemental A_n or binary A_mB_n species, $\text{Ge}_l\text{Si}_m\text{C}_n$ ternary systems are more comprehensive in nature: they provide more opportunities to investigate the bonding characteristics involving all kinds of interactions between different component atoms and therefore better examples to explore the building-up principles applicable in more general situations. But the enormously increasing number of possible low-symmetry isomers lying closely in energies makes complete *ab initio* studies on ternary clusters much more computationally demanding. This difficulty can be dramatically reduced by referring to elemental and binary clusters for which optimized results are available at various theoretical levels.

II. METHODOLOGY

Structural and energy optimizations are performed using a Hartree-Fock calculation followed by configuration interaction (CI) with all single and double (SD) substitutions from the Hartree-Fock (HF) reference determinant with the inclusion of all electrons [CISD (full)]. Both the correlation effect and configuration interaction are explicitly considered in this procedure at an acceptable computational cost. The basis set 6-311G(*d*) is utilized for $s=l+m+n \leq 4$ and a smaller basis 6-31G(*d*) employed for $s=5$ and 6. Frequency analyses are performed at the lowest-energy structures to predict

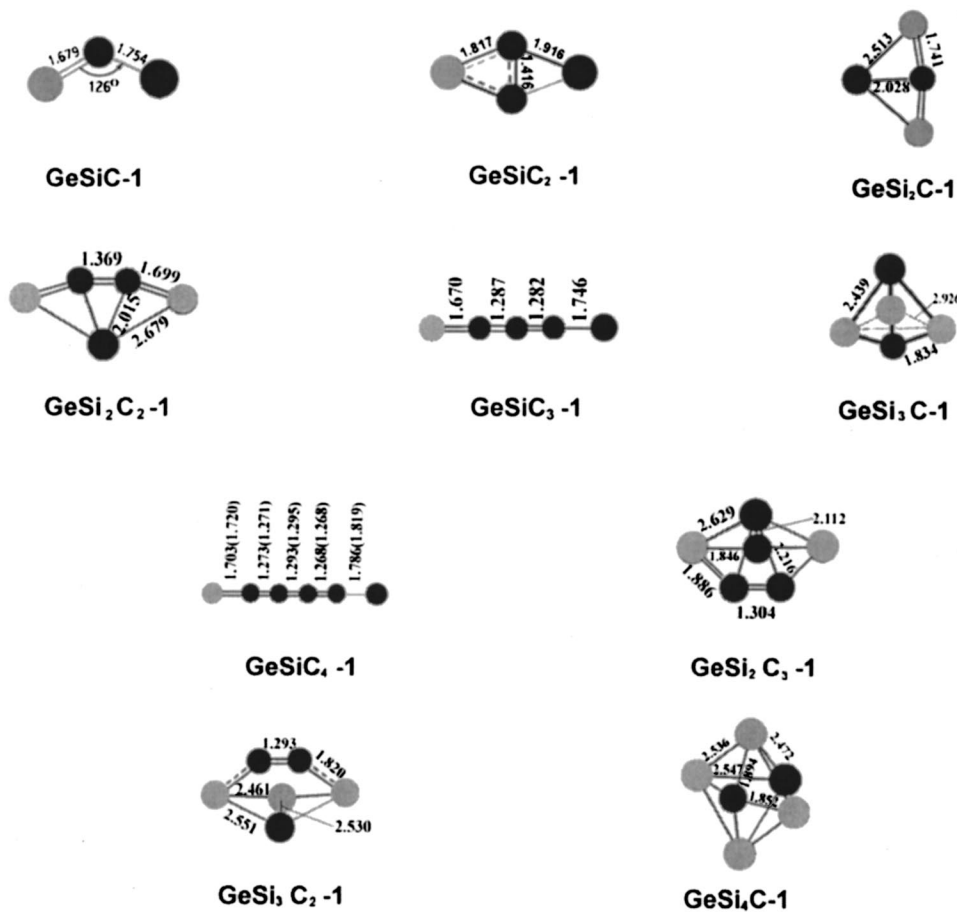
harmonic-vibration frequencies and to check for imaginary frequencies. Initial structures are taken either from the previously published geometries of C_s , Si_s , or Ge_s , or from that of Ge_mSi_n and Si_mC_n by replacing the required number of specific atoms, or arbitrarily constructed based upon chemical intuition to explore the configuration space more extensively. Symmetry constraints are gradually reduced whenever imaginary frequencies are obtained. As open-shell calculations are much more computationally demanding than closed-shell ones, it is fortunate that Si_mC_n and Ge_mSi_n , most $Ge_lSi_mC_n$ semiconductor ternary clusters have singlet ground states except the carbon-rich $GeSiC_4$, which favors a triplet one. The ionization potentials (IP's) of $GeSiC$ and $GeSiC_2$ neutrals and vertical detachment energies (VDE's) of corresponding anions are predicted utilizing the outer valence Green-function (OVGF) frozen-core (FC) method OVGF(FC)/6-311+ $G(2df)$, which has been proved to be fairly accurate in $LiAl_4^-$.¹² All calculations are performed utilizing the GAUSSIAN98 package.¹³

III. STRUCTURAL AND ELECTRONIC PROPERTIES

The low-energy structures of singlet ternary microclusters $Ge_lSi_mC_n$ obtained at CISD (full) are shown in Figs. 1(a) and 1(b) and the corresponding electronic properties tabulated in Table I. Bond lengths obtained for triplet linear $GeSiC_4$ at the DFT- $B3LYP/6-311G(3df)$ level are also shown in parentheses in Fig. 1(a) for comparison.

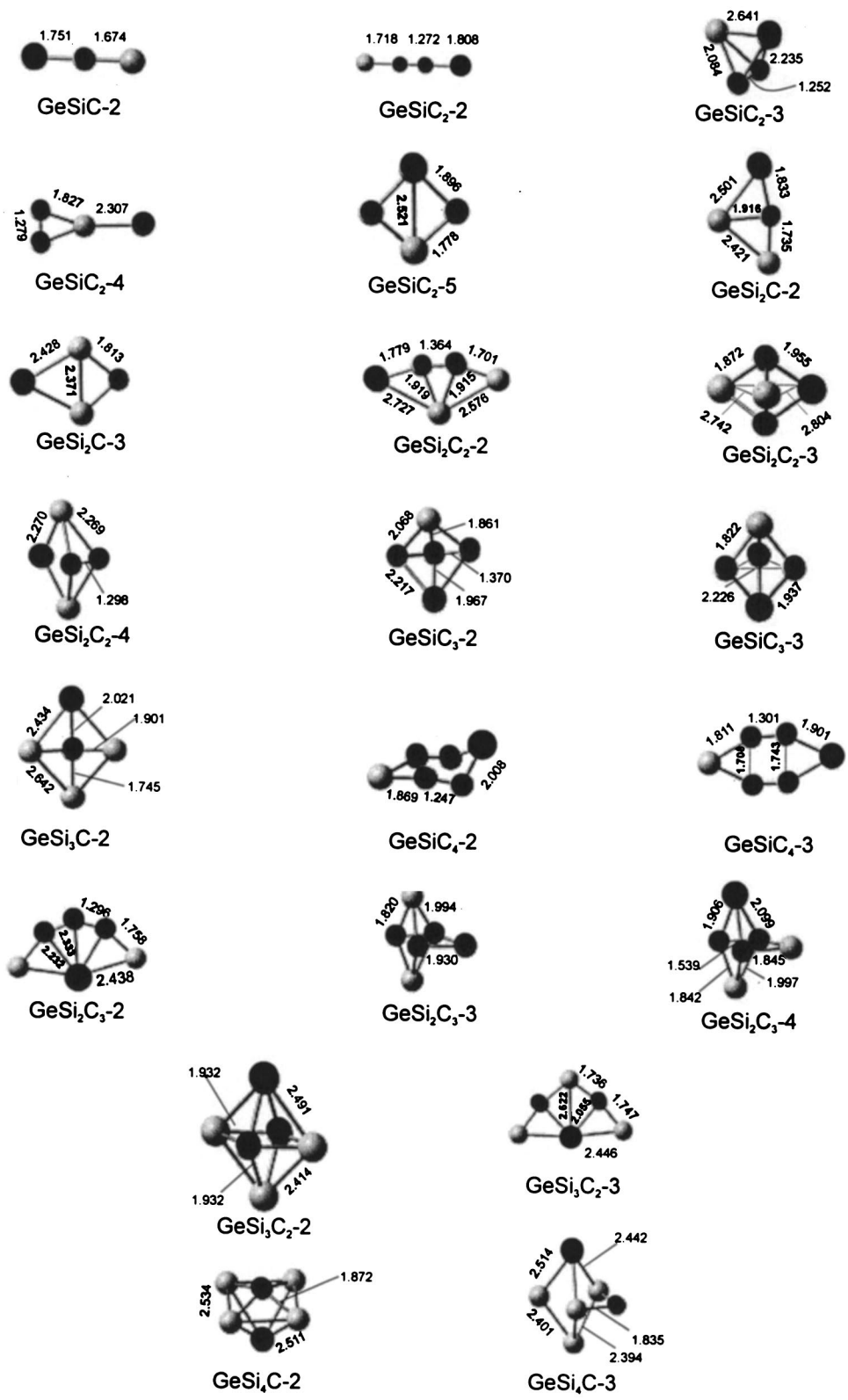
A. Dimers: $GeSi$, GeC , and SiC , and trimer $GeSiC$

To explore the structural growth pattern of ternary systems, we start at dimers. Similar to single species Ge_2 , Si_2 , and C_2 , $GeSi$, GeC , and SiC dimers possess triplet ground states¹² with bond lengths 2.202, 1.825, and 1.716 Å, bond energies 1.23, 2.17, and 3.02 eV, HOMO-LUMO energy gaps of 6.67, 7.63, and 7.88 eV, and stretching vibration frequencies of 467, 708, and 905 cm^{-1} , respectively. AB dimers follow a bond energy order of $C-C > C-Si > C-Ge > Si-$



(a) Lowest-energy structures

FIG. 1. Optimized lowest-energy structures (a) and some of the low-energy isomers (b) of $Ge_lSi_mC_n$ ternary clusters ($s = l + m + n \leq 6$) with important bond parameters indicated at CISD (FULL) level. The big dark balls stand for Ge, gray ones for Si, and the smaller black ones for C.



(b) Some of the lower-energy structures

FIG. 1. (Continued).

TABLE I. Calculated energies E_i (Hartree/particle) or energy differences ΔE_i (eV/particle) relative to the lowest-energy singlet state, HOMO energies E_{HOMO} (eV), HOMO-LUMO energy gaps E_{gap} (eV), and stabilization energies E_{stab} (eV/particle) of some low-energy isomers of $\text{Ge}_l\text{Si}_m\text{C}_n$ at the CISD(full)/6-311G(*d*) level for $s = l + m + n \geq 4$ and at the CISD(full)/6-31G(*d*) level for $s = 5$ and 6.

Cluster	Structure	Symmetry	State	$E_i/\Delta E_i$	E_{HOMO}	E_{gap}	E_{stab}
GeSiC	GeSiC-1	C_s	$^1A'$	-2402.733 385	9.170	9.491	6.962
	GeSiC-2	$C_{\infty v}$	$^1\Sigma_g$	+0.015	8.910	9.041	6.946
GeSiC ₂	GeSiC ₂ -1	C_{2v}	1A_1	-2440.674 642	9.223	9.218	11.29
	GeSiC ₂ -2	$C_{\infty v}$	$^1\Sigma_g$	+0.867	6.366	5.532	10.42
	GeSiC ₂ -3	C_s	$^1A'$	+1.920	7.885	7.273	9.366
	GeSiC ₂ -4	C_{2v}	1A_1	+2.623	7.638	6.041	8.663
	GeSiC ₂ -5	C_{2v}	1A_1	+5.624	7.940	6.856	5.661
	GeSi ₂ C	GeSi ₂ C-1	C_{2v}	1A_1	-2691.848 387	7.741	7.712
GeSi ₂ C	GeSi ₂ C-2	C_s	$^1A'$	+0.289	7.819	7.660	9.096
	GeSi ₂ C-3	C_{2v}	1A_1	+2.670	7.853	6.847	6.716
	GeSi ₂ C ₂	GeSi ₂ C ₂ -1	C_{2v}	1A_1	-2727.165 009	7.086	7.585
GeSi ₂ C ₂	GeSi ₂ C ₂ -2	C_s	$^1A'$	+0.299	6.956	7.480	15.52
	GeSi ₂ C ₂ -3	C_{2v}	1A_1	+1.352	9.192	9.196	14.47
	GeSi ₂ C ₂ -4	C_{2v}	1A_1	+3.829	7.194	5.915	11.99
	GeSiC ₃	GeSiC ₃ -1	$C_{\infty v}$	$^1\Sigma_g$	-2476.105 336	7.843	7.515
GeSiC ₃	GeSiC ₃ -2	C_s	$^1A'$	+3.153	8.118	7.188	14.93
	GeSiC ₃ -3	C_{3v}	1A_1	+7.165	9.050	6.798	10.92
	GeSi ₃ C	GeSi ₃ C-1	C_{3v}	1A_1	-2978.210 938	7.991	7.917
GeSi ₃ C	GeSi ₃ C-2	C_s	$^1A'$	+0.406	7.271	7.399	12.79
	GeSiC ₄	GeSiC ₄ -1	$C_{\infty v}$	$^1\Sigma_g$	-2514.000 317	6.308	5.372
GeSiC ₄	GeSiC ₄ -2	C_s	$^1A'$	+0.117	9.538	9.089	21.77
	GeSiC ₄ -3	C_{2v}	1A_1	+1.322	7.591	8.142	20.57
	GeSi ₂ C ₃	GeSi ₂ C ₃ -1	C_s	$^1A'$	-2765.079 463	8.645	9.965
GeSi ₂ C ₃	GeSi ₂ C ₃ -2	C_{2v}	1A_1	+0.891	6.718	7.304	19.28
	GeSi ₂ C ₃ -3	C_{2v}	1A_1	+0.897	9.586	10.59	19.27
	GeSi ₂ C ₃ -4	C_s	$^1A'$	+1.020	9.803	11.01	19.15
	GeSi ₃ C ₂	GeSi ₃ C ₂ -1	C_s	$^1A'$	-3016.166 903	7.844	8.289
GeSi ₃ C ₂	GeSi ₃ C ₂ -2	C_{2v}	1A_1	+0.920	9.337	9.928	17.75
	GeSi ₃ C ₂ -3	C_{2v}	1A_1	+4.358	5.487	3.982	14.31
	GeSi ₄ C	GeSi ₄ C-1	C_{2v}	1A_1	-3267.230 334	8.246	8.809
GeSi ₄ C	GeSi ₄ C-2	C_{4v}	1A_1	+0.001	8.247	8.802	16.51
	GeSi ₄ C-3	C_s	$^1A'$	+2.909	8.246	7.462	13.60

$\text{Si} > \text{Si-Ge} > \text{Ge-Ge}$, the same as that with DFT.² It represents, at first approximation, the relative *A-B* bond strengths in qualitatively predicting the relative stabilities of various binary or ternary isomers with different numbers of *A-B* interactions. Clusters with specific compositions prefer, in thermodynamic principles, geometries with the maximum numbers of relatively stronger bonds in order to gain the maximum stabilization energies. This principle works well in binary systems.^{2,4-10} Its validity in ternary clusters will be discussed in detail in the following sections.

GeSiC, the smallest ternary cluster, is found to have the singlet bent GeSiC-1 (C_s , $^1A'$) ground-state structure, with the Si=C interaction distance shorter than the typical Si=C double bond length of 1.766 Å.^{9,10} To further optimize this bent structure, we used a bigger basis of 6-311+*G*(*d*) including diffuse functions for C, Si, and Ge atoms.¹³ The optimized geometry is only slightly changed, with the bond

angle decreased to 123.5° and Ge-C and Si-C bond lengths increased to 1.756 and 1.681 Å, respectively. The ground-state structure of GeSiC is close to that of the singlet Si₂C, which was found to have a Si-C-Si bond angle of 120.4° and a Si-C bond length of 1.686 Å.⁸ The singlet linear GeSiC-2 in Fig. 1(b) is a local minimum at CISD/6-311G(*d*) with the lowest frequency of 17 cm⁻¹, but it turned out to be a transition state with a degenerate imaginary (*i*) frequency of 28i cm⁻¹ at CISD/6-311+*G*(*d*). Various calculations confirm that singlet linear geometry is a second-order stationary point on the potential-energy surface of GeSiC. Figure 2 shows the total-energy variation of singlet bent GeSiC with the Ge-C-Si bond angle varying from 110° to 145° (with the bond lengths fixed at $r_{\text{Ge-C}} = 1.754$ and $r_{\text{Si-C}} = 1.679$ Å, respectively). It clearly shows that GeSiC possesses a global minimum with the bond angle between 115° and 130° at MP2, MP3, and CISD levels, but at the HF level this bent geometry disap-

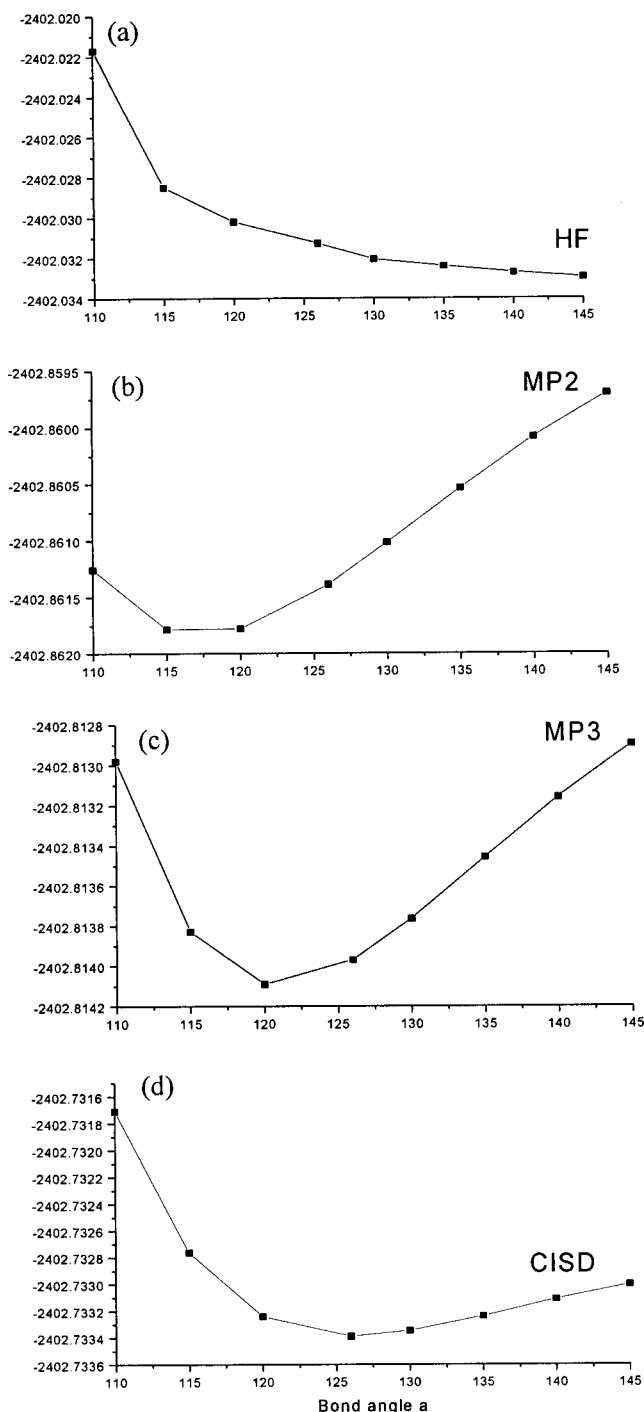


FIG. 2. Energy variation of the bent GeSiC with Ge-C-Si bond angle α at HF (a), MP2 (b), MP3 (c), and CISD (d) levels.

pears. This result clearly shows the importance of including electron correlation effects during structural optimizations. It should also be pointed out that the CISD curve is flatter than both MP2 and MP3 curves in the global minimum vicinities and the CISD curve gradually approaches the energy of the linear structure when the bond angle approaches 180° . Considerable improvement can be achieved with the inclusion of the configuration interaction in the total-energy calculation.

B. Tetramers: GeSi_2C_2 and GeSi_2C

Similar to Si_2C_2 and Ge_2C_2 ,^{2,9,10} the global minimum of the first carbon-rich ternary cluster GeSiC_2 is the rhombic $\text{GeSiC}_2\text{-1}$ (C_{2v} , 1A_1). The C-C bond length 1.416 Å is practically the same as the C-C distance of 1.415 Å in rhombic Si_2C_2 at HF 6-31G* (Ref. 9) and close to the corresponding value of 1.453 Å in the same molecule at MP2/6-31G*.¹⁰ The close similarity between GeSiC_2 and Si_2C_2 indicates that, similar to Si_2C_2 , a multiple bonding character^{9,10} exists in GeSiC_2 between the two transannular tricoordinated C atoms as shown in Fig. 1(a). Orbital analyses show that the high stability of this planar structure originates from its doubly occupied orbital HOMO-3 (B_1), which is a delocalized four-center-two-electron π orbital consisting of p_z contributions mainly from the two transannular carbons and, to a less extent, from the diagonal Si and Ge. It should be mentioned that, according to the orbital coefficients obtained, Si contributes more in HOMO-3 than does Ge, implying that this planar structure is half “aromatic” as shown in Fig. 1(a). Next to the global minimum lies 0.867-eV higher the singlet linear isomer $\text{GeSiC}_2\text{-2}$ with Ge and Si atoms at terminal positions. It is confirmed to be 0.523-eV lower than the triplet linear structure at $B3LYP/6\text{-}31G(3df)$. Both the trans- and cis-chains are converted into the linear geometry automatically during structural optimization. As expected, C_s tetrahedron $\text{GeSiC}_2\text{-3}$, the first three-dimensional species of the ternary system, lies much higher in energy, in line with the expectation that semiconductor tetramers strongly favor planar structures. The C_{2v} three-membered ring structure $\text{GeSiC}_2\text{-4}$ is confirmed to be 2.623-eV above the ground state, while the C_{2v} rhombus $\text{GeSiC}_2\text{-5}$, which has a short Ge-Si diagonal, is found to lie even higher in energy. The weak Ge-Si diagonal interaction cannot compensate the loss of diagonal C-C interaction in energy.

The first Si-rich tetramer GeSi_2C possesses the global minimum of the distorted rhombus $\text{GeSi}_2\text{C-1}$ (C_{2v} , 1A_1) featured with two short Si=C double bonds and a weak Ge-C diagonal interaction. It lies 0.289 eV lower than the Si-C diagonally weakly bonded rhombus $\text{GeSi}_2\text{C-2}$ and 2.670-eV lower than the Si-Si diagonally bonded rhombic $\text{GeSi}_2\text{C-3}$ (C_{2v}). The extra stability of high-symmetry $\text{GeSi}_2\text{C-1}$ over $\text{GeSi}_2\text{C-2}$ comes from the bonding difference between the two structures: the former structure possesses two effective Si=C edge interactions, while the latter has one short Si=C edge bond and one relatively longer Ge-C interaction. The much weaker transannular Si-C interaction in the latter cannot make up the energy loss caused by less Si-C edge interactions. This situation is therefore in line with the bond strength order obtained from dimers.

C. Pentamers: GeSi_2C_2 , GeSiC_3 , and GeSi_3C

A similar situation happens to pentamer GeSi_2C_2 , which is confirmed to have a fan-shaped global minimum—the planar pentagon $\text{GeSi}_2\text{C}_2\text{-1}$ (C_{2v} , 1A_1) characterized with a strong C=C bond and two symmetrically arranged short Si=C interactions. This Ge-tetracoordinated structure has

similar bond parameters compared to the ground-state structure of the C_{2v} planar pentagon Si_3C_2 at the MP2 level.⁷ It is 0.299-eV lower than C_s $GeSi_2C_2$ -2, 1.352-eV lower than C_{2v} $GeSi_2C_2$ -3, and 3.829-eV lower than C_{2v} $GeSi_2C_2$ -4. It is more stable than $GeSi_2C_2$ -2 for the reason that it has one more effective Si=C edge interaction than does the latter. The Si=C bonds in $GeSi_2C_2$ -1 are similar to corresponding Si=C interactions in Si_3C_2 which have the shared-electron number of 2.45, equivalent to almost triplet bonds.⁷ The extra stability of $GeSi_2C_2$ -1 results from its HOMO, which is a delocalized five-center-two-electron π orbital (A_2) involving mainly p_z participation from all the five atoms and makes the planar pentagon molecule "aromatic."

The ground state of C-rich $GeSiC_3$ is the singlet linear $GeSiC_3$ -1, which lies 1.437-eV lower than corresponding triplet linear structure at the DFT-*B3LYP*/6-311G(3*df*) level. It is the first linear ground-state structure obtained in this work. The linear arranged C=C=C, which forms a cumulene-like isomer with a delocalized multicentered π bond, is favored most in energy. Both trans- and cis-chain structures are converted into the linear chain automatically during structural optimization. C_s $GeSiC_3$ -2, a distorted trigonal bipyramid (C_s) containing two effective C-C interactions in the equatorial plane, lies 3.153-eV higher than the ground state, while the regular trigonal bipyramid $GeSiC_3$ -3 (C_{3v}) with a non-C-C bond in the equatorial plane is even less stable. We conclude that the formation of the centered C=C=C chain predominates the relative stability of different $GeSiC_3$ isomers and only a linear arrangement of Si and Ge at terminal positions can best fit the bonding requirement of this carbon-rich species.

In disagreement with $GeSiC_3$, the silicon-rich $GeSi_3C$ clearly favors the trigonal bipyramid $GeSi_3C$ -1 (C_{3v} , 1A_1) over all the other planar and linear structures, with the bond parameters close to that obtained for trigonal bipyramid Si_4C at the MP2 level.⁴ Next to it lies the C_s distorted bipyramid structure $GeSi_3C$ -2, which has the C atom located at the apex position of the equatorial triangle. The three strong Si-C bonds in $GeSi_3C$ -1 make this high-symmetry structure most stable.

D. Hexamers: $GeSiC_4$, $GeSi_2C_3$, $GeSi_3C_2$, and $GeSi_4C$

For ternary hexamers, there are great numbers of possible isomers and frequency analyses are much more time consuming. We choose to optimize some of the initial structures that most possibly produce the ground-state geometries through structural optimizations by referring to Si_4C_2 , Si_2C_4 , and Si_3C_3 .^{5,6}

Hexamer $GeSiC_4$ has the triplet linear $GeSiC_4$ -1 ground-state geometry. It is the only triplet ground state obtained for $Ge_1Si_mC_n$ clusters in the size range studied. Again, it is the C=C=C=C linear chain that makes this cumulene-like molecule most stable over all the other two- and three-dimensional structures. The second lowest-energy isomer is the three-dimensional chair $GeSiC_4$ -2 (C_s), which lies slightly higher than the linear chain. The C_{2v} planar hexagon $GeSiC_4$ -3 is the third in relative stability order, lying 1.322-eV higher than the linear arrangement.

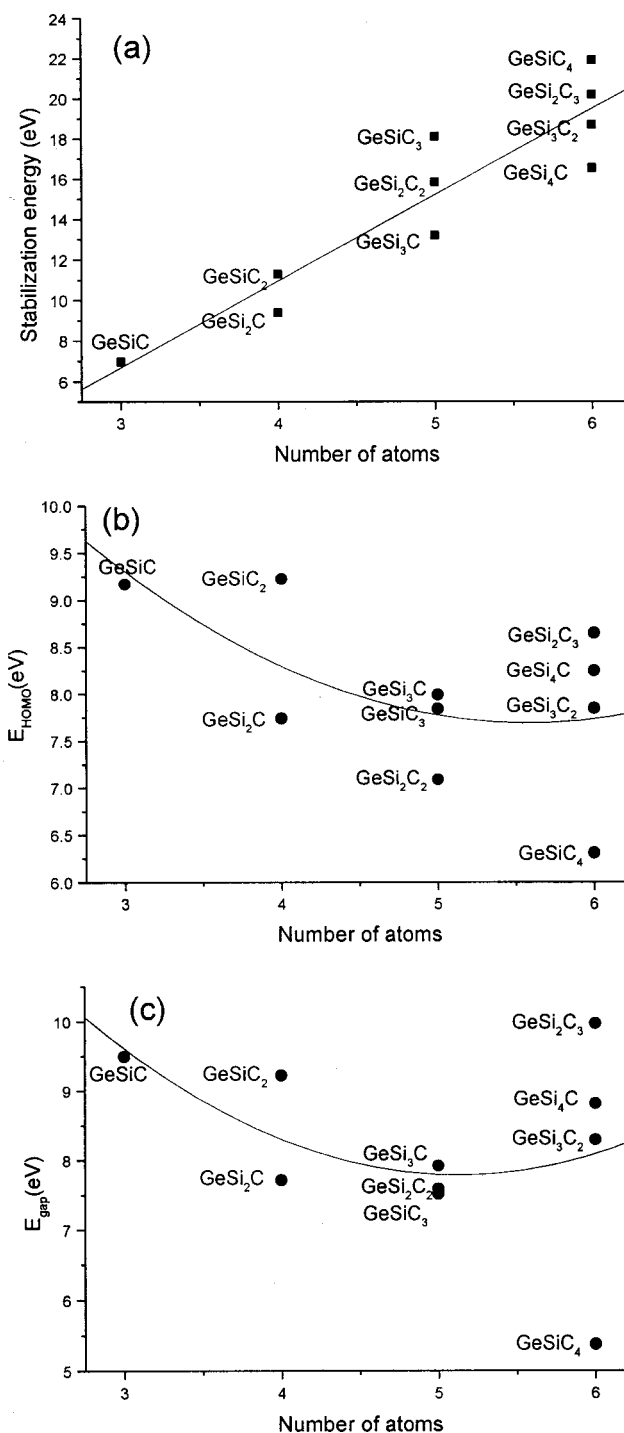


FIG. 3. Variation of stabilization energies E_{stab} (a), HOMO energies E_{HOMO} (b), and HOMO-LUMO energy gaps E_{gap} (c) of the lowest-energy singlet structures obtained for $Ge_7Si_mC_n$ with cluster sizes $s = l + m + n \leq 6$. The linear fit in (a) and quadric fits in (b) and (c) are drawn to guide the eye.

$GeSi_2C_3$ contains equal numbers of carbon and noncarbon atoms. The lowest-energy structure turned out to be the bi-capped tetrahedron $GeSi_2C_3$ -1 (C_s , $^1A'$) with two capping Si atoms. It has an exceptionally wide HOMO-LUMO gap of 9.965 eV and a high estimated ionization potential of 8.645

TABLE II. The calculated five low-lying ionization potentials (IP's, eV) of GeSiC and GeSiC₂ neutrals and vertical detachment energies (VDE's, eV) of GeSiC⁻ and GeSiC₂⁻ anions at the OVG(FC)/6-311 + G(2df) level. The orbital representations and pole strengths are quoted in parentheses.

IP's		VDE's	
GeSiC	GeSiC ₂	GeSiC ⁻	GeSiC ₂ ⁻
9.10 (A', 0.89)	8.94 (B ₂ , 0.89)	1.23 (Σ, 0.91)	1.27 (B ₁ , 0.92)
9.24 (A', 0.88)	9.12 (A ₁ , 0.88)	3.40 (π, 0.88)	3.20 (B ₂ , 0.89)
9.34 (A'', 0.89)	9.74 (A ₁ , 0.89)	3.46 (Σ, 0.89)	3.34 (B ₂ , 0.90)
11.79 (A', 0.83)	11.52 (B ₁ , 0.89)	3.56 (π, 0.88)	3.82 (A ₁ , 0.87)
14.99 (A', 0.72)	12.67 (A ₁ , 0.85)	3.59 (π, 0.86)	3.88 (A ₁ , 0.89)

eV compared to other stable hexamers. It contains a C=C double bond in the bottom plane and the two capping Si atoms lie almost within that plane. It should be noticed that the planarity of the bottom five atoms is almost perfectly

maintained in GeSi₂C₃-1. The fan-shaped planar GeSi₂C₃-2, with a pentacoordinated Ge atom at the center, lies 0.891-eV higher. The Ge-bridging trigonal bipyramid GeSi₂C₃-3 (C_{2v}) lies 0.123-eV lower than the Si-bridging bipyramid

TABLE III. Calculated harmonic vibrational frequencies (cm⁻¹) of the lowest-energy structures of Ge_sSi_mC_n ternary clusters at the CISD(full) level with a 6-311G(d) basis for s=l+m+n≥4, 6-31(d) basis for s=5, and at CISD(FC)/6-31(d) for s=6, with corresponding IR intensities (km/mol) quoted in parentheses. Frequencies for triplet linear GeSiC₄ are calculated at the B3LYP/6-311(3df) level at DFT optimized structures.

Structure	ω ₁	ω ₂	ω ₃	ω ₄	ω ₅	ω ₆	ω ₇	ω ₈	ω ₉	ω ₁₀	ω ₁₁	ω ₁₂	ω ₁₃
GeSiC-1	A'	A'	A'										
6-311G(d)	87	741	1298										
6-311+G(d)	96	754	1282										
	(1)	(37)	(463)										
GeSiC ₂ -1	B ₁	B ₂	A ₁	A ₁	B ₂	A ₁							
	198	337	424	984	990	1223							
	(7)	(61)	(3)	(347)	(0)	(1)							
GeSi ₂ C-1	B ₂	A ₁	B ₂	A ₁	A ₁	B ₂							
	175	253	278	540	627	1194							
	(0)	(1)	(8)	(61)	(36)	(80)							
GeSi ₂ C ₂ -1	B ₂	B ₁	A ₁	A ₁	A ₂	B ₂	A ₁	B ₂	A ₁				
	155	155	171	447	468	602	641	1068	1580				
	(0)	(2)	(0)	(21)	(0)	(71)	(19)	(65)	(2)				
GeSiC ₃ -1	Π	Π	Π	Π	Σ _g	Π	Π	Σ _g	Σ _g	Σ _g			
	99	99	293	293	397	864	864	918	1662	2126			
	(3)	(3)	(0)	(0)	(4)	(32)	(32)	(251)	(2)	(5817)			
GeSi ₃ C-1	E	E	E	E	A ₁	A ₁	A ₁	E	E				
	227	227	248	248	272	344	675	760	760				
	(1)	(1)	(9)	(9)	(5)	(27)	(25)	(27)	(27)				
GeSiC ₄ -1	Π	Π	Π	Π	Σ _g	Π	Π	Π	Π	Σ _g	Σ _g	Σ _g	Σ _g
	62	62	169	169	314	357	357	540	540	661	1217	1872	2019
	(1)	(1)	(0)	(0)	(1)	(7)	(7)	(0)	(0)	(12)	(1)	(82)	(12)
GeSi ₂ C ₃ -1	A'	A''	A'	A''	A'	A'	A''	A'	A'	A''	A''	A'	
	204	221	278	304	371	489	509	567	689	693	991	1720	
	(4)	(2)	(4)	(1)	(23)	(17)	(33)	(69)	(8)	(98)	(49)	(1)	
GeSi ₃ C ₂ -1	A'	A'	A''	A'	A'	A'							
	144	166	249	320	354	368	410	443	533	616	835	1743	
	(3)	(2)	(1)	(10)	(12)	(18)	(7)	(3)	(52)	(18)	(117)	(3)	
GeSi ₄ C-1	A ₁	B ₁	B ₂	A ₁	B ₁	B ₂	A ₂	A ₁	A ₁	A ₁	B ₂	B ₁	
	27	106	121	266	296	318	340	432	462	593	807	892	
	(0)	(0)	(0)	(0)	(5)	(3)	(0)	(0)	(60)	(28)	(67)	(56)	

$\text{GeSi}_2\text{C}_{3-4}$ (C_s) because it possesses stronger Si-C interactions than the latter.

As a carbon-poor species, GeSi_3C_2 possesses the C=C bridged butterfly ground-state structure $\text{GeSi}_3\text{C}_2-1$ (C_s , $^1A'$) with the Si-C interactions exhibiting multiple bonding character as shown in Fig. 1(a). The distorted tetragonal bipyramid $\text{GeSi}_3\text{C}_2-2$ (C_{2v}), which lacks a strong C=C interaction, is found to be 0.920-eV higher than the ground state though it has more Si-C and Ge-C interactions than the ground state. $\text{GeSi}_3\text{C}_2-3$, a fan-shaped planar pentagon with two fused $\text{GeSi}_2\text{C}-1$'s along one edge, turned out to be 4.358-eV less stable than the ground state. $\text{GeSi}_3\text{C}_2-1$ is similar to the C_{2v} Si_4C_2 reported in Ref. 5 in geometries.

It is easy to construct the tetragonal bipyramid $\text{GeSi}_4\text{C}-2$ (C_{4v} , 1A_1) for silicon-rich GeSi_4C . However, frequency analysis indicates that this high-symmetry structure is a first-order stationary point with an imaginary frequency at $35i$ cm^{-1} (B_2). Further optimization with a lower symmetry of C_{2v} leads to the slightly distorted bipyramid $\text{GeSi}_4\text{C}-1$ (1A_1), which is, in fact, an interlinked structure of two rhombic $\text{GeSi}_2\text{C}-1$ (C_{2v}) subunits arranged in directions perpendicular to each other. The extra stability of $\text{GeSi}_4\text{C}-1$ comes from the rhombic subunit $\text{GeSi}_2\text{C}-1$, which is the most stable isomer of GeSi_2C discussed in Sec. III B. However, the distortion is slight and the energy difference (0.001 eV) is small. $\text{GeSi}_4\text{C}-3$, a derivative of bipyramid GeSi_4 by adding a bridging C atom, is found to be 2.909-eV less stable than the ground state.

E. Stabilization energies and HOMO-LUMO energy gaps

Stabilization energies of the lowest-energy structures relative to individual triplet neutral atoms are distributed in two groups around the fitted straight line shown in Fig. 3(a): the carbon-rich species with higher stabilities above the fitted line and the silicon-rich ones below that. High stabilities of C-rich species are attributed to the formation of more effective C=C bond(s) in these systems, which are much stronger than all the other kinds of interactions existing in the ternary systems. HOMO energies of the lowest-energy states, which approximate the first ionization potentials of corresponding clusters according to Koopman's theorem, are shown in Fig. 3(b). HOMO-LUMO energy gaps are also comparatively depicted in Fig. 3(c). Generally speaking, the two figures have close similarities for the reason that LUMO energies are exclusively much smaller than corresponding HOMO energies in values. It is noticed that, in most cases, the carbon-rich species lie below or near the fitted quadric lines except GeSiC_2 and GeSi_2C_3 , which have wider HOMO-LUMO gaps and lower HOMO energies than their neighbors of the same sizes.

F. Ionization potentials and vertical detachment energies

Table II summarizes the predicted five low-lying IP's and VDE's for GeSiC and GeSiC_2 systems based upon the MP2(full)/6-311+ $G(d)$ structures which are close to the global minima shown in Fig. 1(a). It is obvious that OVGE

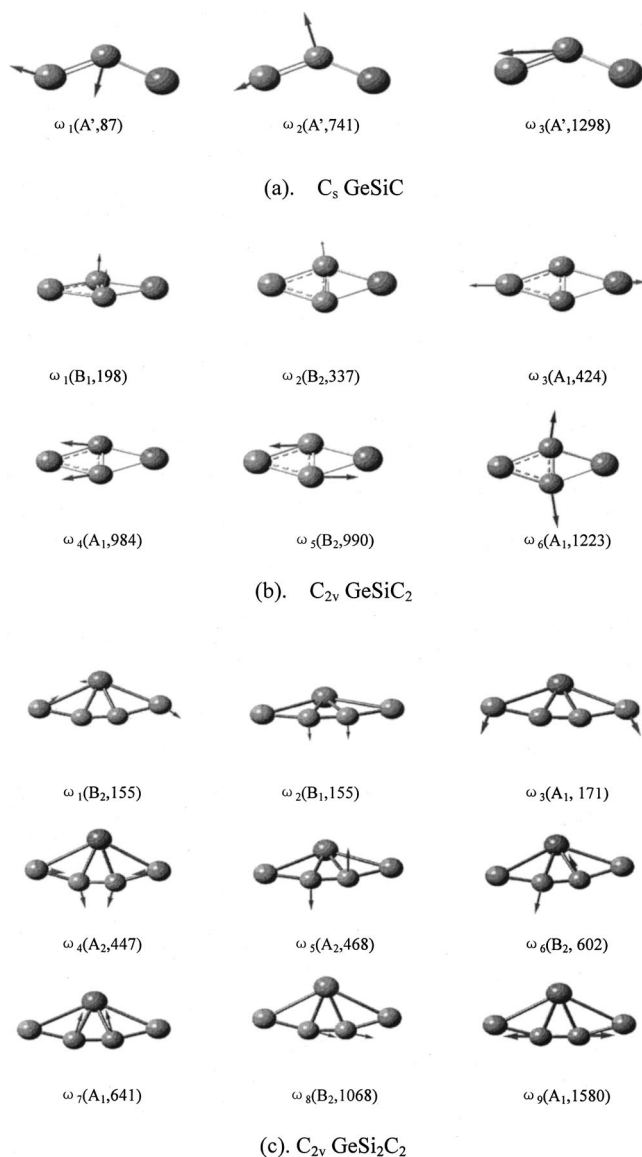


FIG. 4. Harmonic-vibrational modes of the bent GeSiC (a), rhombus GeSiC_2 (b), and the fan-shaped GeSi_2C_2 (c), with symmetries and vibrational frequencies indicated in parentheses.

IP's are lower than the E_{HOMO} values in Table I, which, in Koopmans theorem, approximate the first ionization potentials of the same systems. These predictions would provide useful references for future photoionization threshold measurements and photoelectron spectroscopy studies of semiconductor ternary clusters.

IV. VIBRATIONAL MODES AND FREQUENCIES

Table III tabulates the calculated vibrational frequencies and infrared (IR) intensities of the lowest-energy structures obtained at the same theoretical levels as that used in the optimization processes for $s \leq 5$ and at the CISD (FC) approximation for $s = 6$. Figure 4 shows, as examples, the vibrational modes of $\text{GeSiC}-1$, GeSiC_2-1 , and $\text{GeSi}_2\text{C}_2-1$.

Of the three in-plane vibrational modes of bent GeSiC , ω_2

and ω_3 are infrared active and carbon dominated in terms of amplitudes. The Ge atom, which almost doubles the total atomic mass of C and Si, vibrates in very small amplitudes, while Si displaces in medium sizes. The most IR intensive vibrational mode ω_3 , which mainly involves the right-and-left movements of the carbon atom in a direction nearly parallel to the Ge-Si connection line, leads to spontaneous stretching and depressing of Si-C and Ge-C bonds. The second most intensive IR vibration ω_2 , on the other hand, is dominated by up-and-down movements of the carbon in a direction almost perpendicular to the same line. ω_1 is C and Si collectively dominated and actually IR forbidden. In both ω_2 and ω_1 vibrational modes, the carbon atom vibrates across the Si-Ge connection line, further verifying that the linear arrangement is, indeed, a transition state of singlet GeSiC.

In the six vibrational modes of singlet rhombic GeSiC₂, only ω_1 involves atomic displacements perpendicular to the rhombic plane, while all the others belong to in-plane vibrations. Most vibrational modes are mainly carbon dominated with a certain extent of silicon participation except ω_3 , which mainly involves stretching and depressing of the molecule along the Si-Ge diagonal collectively dominated by vibrations of the two atoms. The highest frequency ω_6 almost exclusively involves vibrations of the two C atoms along the short diagonal and relates GeSiC₂-1 and GeSiC₂-5 structures through the so-called stretching mechanism.¹⁰ The most intensive IR vibration ω_4 mainly represents a collective movement of the two transannular C atoms in the directions practically parallel to the Ge-Si diagonal, resulting in spontaneous stretching and depressing of two pairs of Ge-C and Si-C bonds. The second strongest IR band ω_2 results from the collective movements of the two C atoms in the directions nearly perpendicular to the Ge-Si diagonal. ω_5 is the only twisting vibration which transfers the molecule between two transchains.

Of the nine vibration modes of the fan-shaped GeSi₂C₂, three are carbon dominated, including ω_5 , ω_6 , and ω_9 . ω_1

and ω_3 are Si and Ge collectively dominated, while ω_2 , ω_4 , ω_7 , and ω_8 mainly belong to mixed vibrations of C and Si. The four strongest IR-active modes include ω_6 , ω_8 , ω_4 , and ω_7 , while ω_9 , ω_2 , ω_3 , and ω_1 are much weaker and ω_5 has an IR intensity of zero.

V. SUMMARY

We have presented an *ab initio* investigation with configuration interactions on Ge_lSi_mC_n ternary clusters. Trimers, tetramers, and GeSi₂C₂ are planar, and the C-rich GeSiC₃ and GeSiC₄ are linear, while all the other Si-rich or Si-and-Ge-rich clusters with $s \geq 5$ atoms prefer three-dimensional structures. In these structures, C atoms are bonded together and Si and Ge atoms distributed to form more effective *A-B* bonds, especially direct Si=C bonds. Most ternary clusters have singlet ground states except GeSiC₄ which favors a triplet one. Formation of strong C=C bond(s) predominates the relative stabilities of different isomers for systems with a limited number of C atoms, while Si=C bonds play an important role for silicon-rich species or clusters with close carbon and silicon atomic ratios. Other *A-B* interactions are found to have much weaker influence on cluster geometries. Planar and linear semiconductor clusters are found to possess delocalized multicenter-two-electron π bonds (aromatic) and follow the $(4n+2)$ electron counting rule. Most vibrational modes of small ternary clusters are carbon dominated in terms of amplitudes, while Si atoms vibrate in medium sizes and Ge atoms vibrate very weakly. Further investigations to systematically explore the aromaticity in semiconductor microclusters in both theory and experiments and to predict the ionization potentials and electron affinities of medium-sized semiconductor ternary clusters are in progress.

ACKNOWLEDGMENT

This work has been financially supported by the Natural Science Foundation of Shanxi province with Contract No. 20021029.

¹A. N. Andriotis, M. Menon, and G. E. Froudakis, *J. Cluster Sci.* **10**, 549 (1999).

²S.-D. Li, Z.-G. Zhao, X.-F. Zhao, H.-S. Wu, and Z.-H. Jin, *Phys. Rev. B* **64**, 195312 (2001).

³C. K. Maiti, L. K. Bera, S. Maikap, S. K. Ray, and N. B. Chakrabarti, *Def. Sci. J.* **50**, 299 (2000).

⁴A. D. Zdetsis, G. Froudakis, M. Muhlhauser, and H. Thumel, *J. Chem. Phys.* **104**, 2566 (1996).

⁵M. Muhlhauser, B. Engels, and S. D. Peyerimhoff, *J. Chem. Phys.* **101**, 6790 (1994).

⁶M. Muhlhauser, G. Froudakis, A. Zdetsis, and S. D. Peyerimhoff, *Chem. Phys. Lett.* **204**, 617 (1993).

⁷G. E. Froudakis, M. Muhlhauser, and A. D. Zdetsis, *Chem. Phys. Lett.* **233**, 619 (1995).

⁸R. S. Grev and H. F. Schaefer III, *J. Chem. Phys.* **82**, 4126 (1985).

⁹K. Lammertsma and O. F. Guner, *J. Am. Chem. Soc.* **110**, 5239 (1988).

¹⁰P. V. Sudhakar, O. F. Guner, and K. Lammertsma, *J. Phys. Chem.* **93**, 7289 (1989).

¹¹S.-D. Li, Z.-G. Zhao, H.-S. Wu, and Z.-H. Jin, *J. Chem. Phys.* **115**, 9255 (2001).

¹²X. Li, A. E. Kuznetsov, H.-F. Zhang, A. I. Boldyrev, and L.-S. Wang, *Science* **291**, 859 (2001).

¹³M. J. Frisch, G. W. Trucks, H. B. Schlegel, G. E. Scuseria, M. A. Robb, J. R. Cheeseman, V. G. Zakrzewski, J. A. Montgomery, Jr., R. E. Stratmann, J. C. Burant, S. Dapprich, J. M. Millam, A. D. Daniels, K. N. Kudin, M. C. Strain, O. Farkas, J. Tomasi, V. Barone, M. Cossi, R. Cammi, B. Mennucci, C. Pomelli, C. Adamo, S. Clifford, J. Ochterski, G. A. Petersson, P. Y. Ayala, Q. Cui, K. Morokuma, D. K. Malick, A. D. Rabuck, K. Raghavachari, J. B. Foresman, J. Cioslowski, J. V. Ortiz, B. B. Stefanov, G. Liu, A. Liashenko, P. Piskorz, I. Komaromi, R. Gomperts, R. L. Martin, D. J. Fox, T. Keith, M. A. Al-Laham, C. Y. Peng, A. Nanayakkara, C. Gonzalez, M. Challacombe, P. M. W. Gill, B. Johnson, W. Chen, M. W. Wong, J. L. Andres, C. Gonzalez, M. Head-Gordon, E. S. Replogle, and J. A. Pople, computer code GAUSSIAN98, revision A.6 (Gaussian, Inc., Pittsburgh, PA, 1998).